Science Advances
AAAS

Manuscript Template

Title

- Full title: Differential gene expression and chromatin accessibility in the medial prefrontal cortex associated with individual differences in rat behavioral models of opioid use disorder

Authors

Shirelle X. Liu,[1,2] Peter Muelken,[4] Zia L. Maxim,[1] Aarthi Ramakrishnan,[5] Molly S. Estill,[5] Mark G. LeSage,[1,3,4] John R. Smethells,[3,4] Li Shen,[5] Phu V. Tran,[2] Andrew C. Harris,[1,3,4] and Jonathan C. Gewirtz[1,6*]

Affiliations

[1]Department of Psychology, University of Minnesota, Minneapolis, MN 55455.

[2]Department of Pediatrics, University of Minnesota, Minneapolis, MN 55455.

[3]Department of Medicine, University of Minnesota, Minneapolis, MN 55455.

[4]Hennepin Healthcare Research Institute, Minneapolis, MN 55415.

[5]Icahn School of Medicine at Mount Sinai, New York, NY 10029.

[6]Department of Psychology, Arizona State University, Tempe, AZ 85287.

Abstract

Opioid use disorder (OUD) is a neuropsychological disease that has a devastating impact on public health. Substantial individual differences in vulnerability exist, the neurobiological substrates of which remain unclear. To address this question, we investigated genome-wide gene transcription (RNA-seq) and chromatin accessibility (ATAC-seq) in the medial prefrontal cortex (mPFC) of male and female rats exhibiting differential vulnerability in behavioral paradigms modeling different phases of OUD: Withdrawal-Induced Anhedonia (WIA), Demand, and Reinstatement. Ingenuity Pathway Analysis (IPA) of RNA-seq revealed greater changes in canonical pathways in Resilient (vs. Saline) rats in comparison to Vulnerable (vs. Saline) rats across 3 paradigms, suggesting brain adaptations that might contribute to resilience to OUD across its trajectory. Analyses of gene networks and upstream regulators implicated processes involved in oligodendrocyte maturation and myelination in WIA, neuroinflammation in Demand, and metabolism in Reinstatement. Motif analysis of ATAC-seq showed changes in chromatin accessibility to a small set of transcription factor (TF) binding sites as a function either of opioid exposure (i.e., morphine versus saline) generally or of individual vulnerability specifically. Some of these were shared across the 3 paradigms and others were unique to each. In conclusion, we have identified changes in biological pathways, TFs, and their binding motifs that vary with paradigm and OUD vulnerability. These findings point to the involvement of distinct transcriptional and epigenetic mechanisms in response to opioid exposure, vulnerability to OUD, and different stages of the disorder.

MAIN TEXT

Introduction

Opioid use disorder (OUD) is a neuropsychological disease with profound effects on the individual and society (*1*). The fact that 1-5% of people who are prescribed opioids develop OUD highlights not only their addictive potency, but also the substantial individual variability in susceptibility to their effects (*2–4*). Identifying the molecular mechanisms associated with vulnerability to OUD is critical in developing more effective prevention and treatment strategies.

Given the chronic and relapsing nature of OUD and other drug-use disorders, such mechanisms presumably involve stable, epigenetic changes in gene regulation that affect long-term behavioral outcomes (*5*, *6*). To investigate these mechanisms, the transcriptomic and epigenomic landscape has been mapped in functionally relevant brain regions after rodents have acquired, or relapsed to, drug self-administration (*7–11*). There is considerable clinical and preclinical evidence implicating certain, initial acute responses to addictive drugs (e.g., euphoria, aversion) as being predictive of later vulnerability to addiction (*12–17*). This raises the possibility that some epigenetic markers of addiction may emerge upon initial episodes of exposure to an opioid drug, prior to the manifestation of full-fledged OUD. To the extent that such adaptations exist, it is not clear whether they persist, or whether new epigenetic markers emerge over the course of OUD progression. Resolving these questions has important implications for understanding the etiology of OUD and, potentially, for the development of prophylactics to accompany the use of acute and chronic opioid analgesics.

To this end, we sequenced genomic transcription (using RNA-seq) and chromatin accessibility (using ATAC-seq) across three behavioral paradigms modeling different phases of OUD using the opioid morphine (Fig. 1). To examine epigenomic adaptations in response to initial opioid exposure we utilized withdrawal-induced anhedonia (WIA), indexed as an increase in thresholds for intracranial self-stimulation (ICSS) during spontaneous withdrawal from experimenter-administered morphine. A critical advantage of this behavioral measure is that it predicts multiple measures of subsequent morphine self-administration (MSA) and therefore provides a prospective behavioral model of OUD vulnerability. To investigate the epigenomics of chronic, compulsive drug-taking, we used the behavioral economic measure of demand, which reflects the persistence of drug-taking in the face of increased “cost”. This measure has been validated across species, including in many human studies of addiction to opioids and other drugs (*18*, *19*). Finally, to measure relapse to drug seeking after a period of abstinence we used a cue/drug-induced reinstatement paradigm, the neurobiological substrates of which have been extensively investigated (*20*).

In all three paradigms, we examined the transcriptional and epigenetic effects of opioid versus saline treatment in the rat medial prefrontal cortex (mPFC), as well as differences in these effects as a function of high- versus low-vulnerability to our three OUD-like behavioral phenotypes. We focused on the mPFC based on its critical role in circuitry underpinning all phases of addiction in both humans and rodents (*21–23*). We used relatively large group sizes to provide sufficient power both to conduct between group comparisons based on animals’ phenotypic classification, and to enable the use of statistical approaches that require larger group sizes (*24–26*). Collectively, our findings revealed a variety of epigenetic adaptations in the mPFC that were associated with one or more behavioral paradigms. These adaptions were associated either with opioid exposure/consumption per se, or explicitly with behavioral traits of OUD vulnerability,

with some of the latter appearing to serve a protective function. As such, our findings provide new directions for the discovery of potential treatments for OUD.

Results

Rats showed considerable individual differences in behaviors reflecting vulnerability to OUD-like behavior

Experiment 1: Withdrawal-induced anhedonia (WIA)

Baseline ICSS thresholds and response latencies did not differ between groups (Table S1). A 3-way ANOVA on ICSS thresholds during withdrawal testing indicated a significant main effect of morphine dose (F (1, 35) = 20.3, $p < 0.0001$), reflecting an elevation in ICSS thresholds in morphine-treated compared to saline-treated rats (Fig. 2A), but no significant effects of sex, session, or interactions between these variables. ICSS response latencies were not significantly affected during withdrawal (Fig. S1A), indicating that the ICSS threshold data were not influenced by non-specific (e.g., motoric) effects of morphine exposure.

Experiment 2: Demand

Rats reliably acquired morphine SA, with infusions per day significantly higher in the morphine SA versus saline SA group for both sexes at the end of the acquisition period (Fig. S1B). Analysis of infusions during FR escalation indicated a significant effect of FR value, (F (1.6, 32.3) = 29.4, $p < 0.0001$), but no effect of sex or FR x sex interaction. Comparison of data collapsed across sex indicated that infusions were decreased compared to FR 1 at all FR values ≥ FR 3 (Dunnett q = 2.9 - 6.3, $p < 0.05$ or 0.01; Fig. 1B). Morphine consumption during demand testing was well described by an exponential demand function, with R^2 values typically ≥ 0.85 for individual animals (Table S2) and R^2 = 0.99 for rats as a group (Fig. 1C).

Experiment 3: Reinstatement

Extinction of morphine SA produced a significant reduction in active lever presses (Fig. S2). A 2-factor ANOVA on reinstatement scores indicated no main effect or interaction with to sex, but there was a main effect of training drug (Mor vs Sal; F(1, 36) = 26.86, $p <$ 0.0001; Fig. 1D). Active and inactive lever responding (not figured) was also assessed using a 2-factor ANOVA after the data was collapsed across sexes due to a 3-factor ANOVA that found no main effect or interaction with sex. Specifically, we found a significant interaction of reinstatement condition and lever type (F(1, 50) = 20.63, $p <$ 0.0001)) with a Šidák post-hoc comparison revealing significantly greater responding on only the active lever (t_{24} = 6.855) following Morphine + Cue exposure vs. Saline + No Cue exposure . In the saline control group a 3-factor ANOVA revealed a main effect of lever type (F(1, 11) = 54.00, $p < 0.0001$), but no main effect or interaction with sex. After collapsing across sex, a 2-factor ANOVA a main effect of lever type was observed (F(1, 24) = 46.76, $p < 0.0001$) and a lever type x reinstatement condition (no cue vs. cue) (F(1, 24) = 6.47, $p < 0.05$), with a Šidák post-hoc comparison revealing significantly lower active-lever responding (t_{24} = 3.123) following Sal + Cue exposure vs. Saline + No Cue exposure (data not shown).

Our behavioral data showed a considerable degree of individual variability for all three measures (see z-score distribution in Fig. 1E).

Differences in canonical pathways altered in resilient versus vulnerable male rats

Principal component analysis (PCA) plots of RNA-seq data revealed 15%-23% variations in the top 500 expressed genes among male and female transcriptomes across the three paradigms were explained by drug treatment, whereas 17%-25% of the variations were explained by sex (Fig. S3). Due to strong sex effects, NGS data were analyzed in a sex-separated manner where feasible. Numbers of DEGs in each comparison pair are summarized in Tables S3 and S4. Contrary to our expectations, IPA canonical pathway analysis of these DEGs suggested that a far larger number of biological pathways were altered in resilient compared to vulnerable male rats across all three paradigms (Fig. 3A). Similar trends were also found in female WIA and Reinstatement paradigms, but not in the Demand paradigm (Fig. S4). Top altered canonical pathways were associated with signaling pathways in the nervous system (e.g., CREB, G-protein, cAMP signaling) and inflammation (e.g., S100, phagosome, macrophage, natural killer cell, neutrophil, T lymphocytes, neuroinflammation signaling) (Fig. 2B).

Myelination-related gene networks were implicated in OUD vulnerability with sex-specific patterns

Differential connectivity of genes in WGCNA modules between morphine and saline animals was detected in five modules built with male and female morphine WIA rats. Gene Ontology (GO) analysis revealed a “saddlebrown” module specifically involved in oligodendrocyte functions and myelination that showed decreased connectivity (MeDC = -0.38, $p = 0.02$) in morphine rats (Fig. 4A). ARACNe analyses of genes in the “saddlebrown” module revealed gene networks regulated by two TFs, PRDM8 and HR (Fig. 4B). Both of them function as histone epigenetic modifiers - PRDM8 being a histone methyltransferase and HR being a histone lysine demethylase. PRDM8 specifically regulates oligodendrocyte differentiation (*27*). IPA upstream regulator analysis of gene expression in WIA animals of both sexes predicted changes in activities of two TFs, both of which are important in myelination (*28–30*), TCF7L2 and SOX2, (Fig. 4C, top panel, male; bottom panel, female). Interestingly, these TFs were predicted to be more significantly inhibited in the resilient group in males, yet more significantly activated in the vulnerable group in females. Furthermore, despite the same two TFS being implicated, the two networks shared only five common DEGs between them out of a total of 34 DEGs in males and 26 in females.

Neuroinflammatory responses were dependent on the stages and vulnerability in OUD

Differential connectivity of genes in WGCNA modules between morphine and saline animals was detected in 6 modules built with male and female morphine Demand rats. GO analysis revealed a “white” module showing decreased connectivity (MeDC = -3.81, $p <$ 2.20E-16) in morphine rats that is specifically involved in immune response/inflammation (Fig. 5A). IPA canonical pathway analysis of male and female Demand RNA-seq data corroborated this observation (Figs. 5B). Strikingly, further examinations revealed that resilient male rats showed activation in inflammation-related pathways, whereas vulnerable rats showed a moderate inhibition in the same pathways (Fig. 5B, male). In

female animals, inflammation pathways in resilient individuals remained largely unchanged, and were inhibited in vulnerable individuals (Fig. 5B, female).

Aside from the sex and resiliency, changes in inflammation pathways also varied with paradigms. In males, resilient rats exhibited strong inhibition of inflammation pathways in the WIA paradigm, but activation of the same pathways in the Demand and Reinstatement paradigms, while vulnerable rats in general showed inhibition of these pathways across the three paradigms (Fig. 5C). No specific patterns were observed in females (Fig. S5).

WGCNA metabolic modules were correlated with behavioral vulnerability

Differential connectivity of genes in WGCNA modules between morphine and saline animals was detected in 6 modules built with male and female morphine Reinstatement rats. GO analysis revealed a "darkgreen" module showing decreased connectivity (MeDC = -0.08, p = 0.02) in morphine rats in which there was significant enrichment of genes involved in metabolic processes. A module-trait correlation analysis showed that expression levels of genes in this module were negatively correlated with reinstatement scores in male morphine rats (correlation coefficient -0.6, p = 0.04; Fig. 6A). In addition, modules "darkgreen" (correlation coefficient -0.71, p = 0.01) and "magenta" (correlation coefficient -0.6, p = 0.05) built with Demand male and female morphine animals that were also enriched in metabolism processes were negatively correlated with elasticity of Demand (α) in male morphine rats (Figs. 6B, C).

Variance partitioning analyses revealed genes whose expression varied with vulnerability across the three paradigms

We next performed variance partitioning analyses to investigate transcriptional mechanisms that were shared across different stages of OUD vulnerability. Up to 32% and 36% of the variations in gene expression were explained by vulnerability in male and female morphine animals, respectively (Figs. 7A, B). Heatmaps of the top 50 genes whose expression variation was most explained by vulnerability in males (Fig. 7C) and females (Fig. 7D) showed gene expression patterns clustered with vulnerability. GO analyses of the 754 genes with at least 10% of the variation explained by vulnerability in males revealed these genes were enriched in regulatory processes of gene expression, including nucleus export, chromatin remodeling, and nucleic acid metabolic processes (Fig. 7E). In contrast, GO analyses of the 372 genes with at least 10% of the variation explained by vulnerability in females revealed these genes were enriched in GTPase cycle and signal transduction (Fig. 7F).

RRHO revealed strong correlation of gene expression between vulnerable rats and human OUD patients

To evaluate the translational value of our models, we correlated differential gene expression between our three rat models and that of the dlPFC and NAc from humans with OUD. There was a strong correlation between the late-stage Reinstatement model with both human dlPFC and NAc in both males and females (Figs. 8, S6), with the strongest correlation between male reinstatement model and human NAc (Fig. 8). Once again, these effects were primarily driven by vulnerable animals in both males (Fig. 8A) and females (Fig. 8B).

Chromatin accessibility of top 10 transcription factor binding sites showed paradigm specificity

Numbers of differential sites in each comparison are summarized in Tables S5 and S6. IPA canonical pathway analysis of differential sites between resilient and vulnerable rats showed sex-specific changes in processes including neuroinflammation (S100, phagosome), energy metabolism (insulin signaling), cell signaling (CREB, glutaminergic receptor, calcium, serotonin), and neurodevelopment (GTPase, netrin) (Fig. 9A). HOMER motif analysis revealed distinct TF families associated with differential sites. Among the top 10 significant TFs in males, motifs of members of AP-1 family (e.g., Fos, JunB, Fra, Atf) were significantly enriched in morphine exposed rats in all three paradigms, but not between resilient verses vulnerable groups. In contrast, members of MEF2 (i.e., MEF2a-d) and bHLH (e.g., Atoh1, Npas4) families were also associated with OUD vulnerability. Members of NR family (e.g., PGR, GRE) were specific to the Reinstatement paradigm with no significant differences between resilient verses vulnerable groups, while the T-box family was specifically associated with vulnerability (Fig. 9B).

Discussion

In this study, we evaluated behavioral vulnerability to MSA in male and female rats in 3 paradigms representing different phases along the trajectory of OUD: WIA, Demand, and Reinstatement. We then compared gene transcription and chromatin accessibility across the genome in the mPFC both as a function of drug treatment and individual differences in behavioral outcomes to identify molecular and cellular mechanisms underlying vulnerability to OUD. We discovered key brain processes and epigenetic regulators associated with susceptibility to OUD that are shared and unique to each paradigm, as well as those that differ by sex. These results will provide important insights on the development of more effective and personalized therapeutics for OUD.

Perhaps the most striking and unexpected observation was that gene expression in canonical pathways was more profoundly altered in resilient rats compared to vulnerable rats. We saw this pattern across the three behavioral models in male rats, although it was strongest in the WIA and Reinstatement paradigms. It is commonly believed that the magnitude of dysregulated biological processes upon substance exposure is positively correlated with addiction severity, and that addiction is a result of passive brain maladaptation to the pharmacological effects of addictive substances (*31*, *32*). However, recent studies have also raised the possibility that resilience to substance use disorders might be mediated by mechanisms that are distinct from those contributing to addiction susceptibility (*33*, *34*). Our results, especially in the WIA and the Reinstatement models in both males and females, strongly supported this emerging perspective of OUD vulnerability; namely, that vulnerability to OUD could be the consequence of inadequate compensatory adaptations to the drug as much as, or more than, a consequence of excessive maladaptive responses to the drug. Given evidence that there are distinctive waves of gene expression across the passage of time during abstinence, including changes in the directionality of gene expression (*11*, *35*), it is possible that the relationship between the degree of gene expression in functional pathways and vulnerability would be reversed either in the immediate aftermath of morphine exposure, and/or after longer term abstinence. In either case, our findings highlight the importance of accounting for individual differences in addiction vulnerability at both behavioral and mechanistic levels, and of entertaining the possibility that resilience to OUD is associated with enhanced transcription in addiction-associated functional pathways.

Among gene modules that appear to exhibit inadequate recruitment in vulnerable rats, the most notable to emerge was a network associated with myelination and oligodendrocyte maturation in the WIA paradigm. Specifically, WGCNA revealed reduced connectivity in this network upon morphine treatment. The TF-coding *Prdm8*, which was revealed through ARACNe as having substantial regulatory connections with other genes in the network, is a member of the PRDM TF family that broadly regulate gene activity through chromatin regulation and are themselves regulated through DNA methylation (*36*). PRDM8 in particular is involved in repressing the production of oligodendrocyte precursor cells (*27*). Additionally, at least 28 of the functionally relevant genes in this network are involved in myelin formation (i.e., MAL, MOG, PLP, OPALIN), which occurs at a later stage of oligodendrocyte differentiation.

Consistent with these network analysis findings, a comparison of gene expression in behaviorally vulnerable and resilient males in the WIA paradigm revealed two TFs, TCF7L2 and SOX2, as more strongly inhibited in resilient rats. These TFs positively regulate oligodendrocyte proliferation and differentiation, as well as CNS myelination and remyelination post injury (*28–30*). Interestingly, although sharing only 5 DEGs with the males, TCF7L2 and SOX2 networks were also significantly identified in female rats. In addition, in contrast to the strong inhibitory effects in the resilient males, female animals exhibited stronger activation of those networks in the vulnerable group. Taken together, these results suggest a reduced oligodendroglial and myelination process during withdrawal from the initial morphine exposure to be protective against OUD-like behaviors. Supporting the functional relevance of these correlational effects, a recent report indicates that blockade of oligodendrogenesis in the mouse ventral tegmental area (VTA) reduced dopamine release in the nucleus accumbens and induction of a conditioned place preferences for morphine (*37*). Furthermore, these findings are consistent with reduced white matter in the PFC of rats exposed to oxycodone, and in OUD patients (*38*, *39*)

While resilience was most closely associated with differential activity in oligodendrogenesis-related pathways in the WIA paradigm, resilience in males in the Demand paradigm was most strongly associated with increased activity in gene pathways associated with neuroimmune function. Furthermore, in a striking parallel to the sex differences we saw in the regulation of oligodendroglial activity, female rats showed the same broad directionality as males, except that greater differential activity of the neuroimmune-related gene network was found in resilient animals. This suggests that proinflammatory responses to opioids (*40–42*) may in fact serve a protective function in the domain of opioid addiction liability at the same time that anti-inflammatory responses tend to promote the analgesic effects of opioids (*43*).

To further investigate the existence of a core transcriptional machinery associated with the trait of OUD vulnerability, independent of the idiosyncratic or unique characteristics of each of our three paradigms, we conducted a Variance Partitioning Analysis to estimate the proportion of variance in gene expression attributable to our behavioral phenotype of vulnerability across the three paradigms. This analysis yielded a stronger signal in males than in females, and specifically enrichment of gene pathways associated with various aspects of epigenetic regulation, such as nuclear transport and chromatin remodeling. Two of the 6 genes enriched in the top category (nuclear transport) are the proteins XPO4 (Exportin 4) and RAN (RanGTPase) that form a complex to transport a number of transcription factors in and out of the nucleus and, as recently shown, to export circular RNAs from the nucleus (*44*, *45*). These regulatory RNA molecules have, in turn, been implicated in a number of studies in addiction, including OUD in animal models (*46*, *47*).

Additionally, methylation levels of the XPO4 gene in T Cells, together with those of one other gene, are sufficient to predict mechanical sensitivity in a model of chronic pain (*48*). Collectively, these findings provide initial support for the notion that gene networks associated with regulation of nuclear transport and gene expression may be central to individual differences in vulnerability to OUD.

While providing a comprehensive snapshot of gene transcription at a given moment in time, the character of the transcriptome can vary greatly across both large (weeks) and small (hours) timescales in response to events such as the circadian cycle and transient environmental fluctuations (*49–52*). On the other hand, epigenetic modifications that regulate gene expression, either transiently or in a sustained manner, are likely more tightly associated with long-term behavioral outcomes (*5*). Therefore, we assessed differential chromatin accessibility to TFs in resilient and vulnerable animals across 3 paradigms. AP-1, a TF family that is had been strongly and repeatedly implicated in OUD (*53*), was among the top 10 TFs identified by HOMER motif analysis upon morphine exposure (i.e., morphine vs. saline) but was not differentially enriched in resilient vs. vulnerable rats. This suggests that the AP-1 TF family might primarily respond to the pharmacological effects of morphine rather than behavioral vulnerability to OUD. In contrast, chromatin accessibility of the MEF2 and bHLH TF family binding motifs differed significantly in resilient vs. vulnerable rats, suggesting a specific role in OUD vulnerability.

A further distinction between differentially accessible TF motifs was whether they were implicated in one phase of addiction or across all phases. Thus, whereas the AP1 and MEF2 families were implicated across all three paradigms, bHLH was implicated only in Demand and the Nuclear Receptor (NR) family, e.g., progesterone receptor, glucocorticoid receptor) only in reinstatement. In contrast to the known involvement of AP-1 and MEF2 TF families in addiction-like behavior, the association between bHLH and NR family TFs and opioid addiction vulnerability is novel but coheres with a recent single-nucleus ATAC-seq study implicating both TF families in individual differences in the severity of cocaine self-administration in mice (*54*).

In summary, our results suggest that across three very different behavioral paradigms that are designed to capture different phases of the trajectory of OUD, differential recruitment of functional pathways is greater in animals that are resilient to the addictive effects of opioids. This suggests that vulnerability to OUD, across its trajectory, is attributable in part to a failure to mount adequate counter-adaptational responses to repeated encounters with opioids. These experiments revealed some candidate functional networks and their drivers, such as those mediating oligodendrocyte maturation and inflammatory responses, and a constrained set of candidate transcription factors. Perhaps most notably, we identified an association between functional gene sets contributing to epigenetic regulation, and an underlying trait of OUD vulnerability across the three paradigms. Thus, the current findings suggest several potential avenues aimed towards boosting compensatory responses during opioid withdrawal to mitigate vulnerability to persistent and relapsing OUD.

Materials and Methods

Animals

Experimentally naïve male and female adult Sprague Dawley rats (Inotiv, Lafayette, IN) weighing 275-300 g (male) or 225-250 g (female) at arrival were used. All rats were individually housed in a temperature- and humidity-controlled colony room with unlimited access to water under a reversed 12-h light/dark cycle. All behavioral testing

occurred during the dark (active) phase. Beginning one week following arrival, food was restricted to 18 g/day to facilitate operant performance, avoid detrimental health effects of long-term *ad libitum* feeding, and limit catheter migration in rats tested for MSA. All procedures were approved by the Institutional Animal Care and Use Committee (IACUC) of the Hennepin Health Research Institute and University of Minnesota in accordance with the NIH Guide for the Care and Use of Laboratory Animals and the Guidelines for the Care and Use of Mammals in Neuroscience and Behavioral Research.

Behavioral experiments

Experiment 1: Withdrawal-induced anhedonia

Rats were prepared and trained on a discrete-trial ICSS procedure (see Supplemental Material) in daily ≈ 1-hour sessions conducted Mon-Fri until ICSS thresholds were stable (<10% variability over 5 days). On the first test day, rats were tested for ICSS and then immediately injected with either 5.6 mg/kg morphine sulfate (n = 26, 16 males and 10 females) or saline (n = 13, 8 males, 5 females). ICSS was then tested 23 hours later to measure spontaneous withdrawal, which was expected at this timepoint (*16*, *59*, *60*). All rats were then injected as on the preceding day. This injection regimen was repeated for 11 days, with ICSS tested 23 hours after each injection except for a 2-day weekend break in behavioral testing following the 5th and 6th injections. On these days, injections were administered at their usual time. Immediately after the final ICSS test (24 hours after the final morphine or saline injection), rats were sacrificed and tissue from multiple brain structures was harvested and preserved. This is a standard time point for evaluating effects of drugs or other manipulations on the transcriptome and epigenome (*61–64*). The morphine group was larger than the saline group to allow stratification into high and low WIA groups (see below).

Experiment 2: Demand

Rats were implanted with i.v. catheters and allowed to respond for i.v. infusions of 0.4 mg/kg morphine (n = 23, 11 males, 12 females) or saline (n = 11, 5 males, 6 females) during daily 2-hr sessions conducted 7 days per week using our standard apparatus and procedures (see Supplementary Material). Rats were tested under a fixed ratio (FR) 1 schedule for at least 10 sessions and until robust responding was observed, at which point the FR response requirement was increased to FR 2 for at least 5 sessions. The FR was then increased to FR 3 for at least 10 sessions and until acquisition criteria were met (≥10 infusions per session, ≤20% coefficient of variation, and ≥2:1 response ratio on the active versus inactive lever across 3 sessions). To test demand, the FR requirement was increased each day as follows: FR 1, 2, 3, 6, 12, 24, 48, 96. Morphine consumption under this protocol is well described by the current exponential demand function (*16*, *65*). Twenty-four hours after completion of demand testing, brains were harvested as described in Experiment 1. Rats in the saline group did not acquire stable SA under the FR 3 schedule and therefore were not tested for demand. Brain collection in these animals occurred on the same day as that for a control-paired morphine rat that began the protocol at a similar time.

Experiment 3: Reinstatement

Male and female rats (n = 26, 12 males, 14 females) were implanted with i.v. catheters and allowed to respond for infusions of 0.4 mg/kg/infusion under an FR 1 schedule as described in Experiment 2. Following at least 10 sessions and attainment of stable responding (same stability criteria as described for Experiment 2), extinction conditions were introduced in which active lever responses resulted in saline infusions in the absence of the drug-associated cue light. Extinction was tested for a minimum of 21 sessions and until responding decreased by 75%, or 42 days of extinction, whichever occurred first,

prior to reinstatement testing. During an initial "baseline" session, rats were given a s.c. saline injection 10 minutes prior to the session, and active lever responses continued to deliver saline infusions in the absence of the drug-associated cue light. To test morphine + cue-induced reinstatement, the following day rats were injected s.c. with morphine (1.0 mg/kg) 10 min prior to the session. Active lever presses during that session resulted in saline infusions and the presentation of the drug-associated cue light. Brain samples were collected 24 hours later. This morphine dose has been shown to reliably elicit reinstatement (*16*). Reinstatement was induced by combined exposure to morphine + cue because this condition produces more robust reinstatement than either morphine or the cue alone (*16*). A negative control group (n = 13, 6 males, 7 females) was allowed to respond for i.v. infusions of saline throughout the protocol. To control for the visual stimulus conditions of the morphine group, control rats had saline delivered in the presence of the cue light for the same number of "acquisition" sessions as a control-paired morphine rat. Likewise, the same number of "extinction" sessions were conducted as the control-paired morphine rate and thus, no cue light was produced with saline deliveries. During "reinstatement", the negative control rats were administered s.c. saline 10 min prior to both test sessions, wherein active lever presses had no consequences during the first "baseline" session but would produce the saline-associated cue during the second "reinstatement" test session. Brain samples in these rats were collected 24 hours after the "reinstatement" assessment.

Statistical analysis

Withdrawal-induced anhedonia. ICSS thresholds and response latencies served as the measure of brain reinforcement function and general motoric function, respectively. Baseline ICSS thresholds (in µA) and response latencies (in sec) were defined as the mean during the last five sessions prior to withdrawal testing. These data were analyzed using separate 2-factor ANOVAs with morphine dose (0 or 5.6 mg/kg) and sex as between-subject factors. ICSS thresholds and latencies during withdrawal testing were subsequently expressed as a percentage of baseline and analyzed using a 3-factor ANOVA with morphine dose and sex as between-subject factors and session as a within-subject factor. Rats were assigned to High and Low WIA groups based on a median split of average ICSS thresholds (% baseline) across all test sessions.

Demand. Infusions per day during the last 5 sessions of acquisition were compared using 3-factor ANOVA with morphine unit dose (0 or 0.4 mg/kg/infusion) and sex as between-subject factors and session as a within-subject factor. Infusions at each FR during demand testing in the morphine group were compared using a one-factor ANOVA with the FR requirement as a within-subject factor, followed by Dunnett's post hoc tests comparing infusions at FR 1 to those at subsequent FRs. To measure demand, exponential demand curve analyses were conducted as described in the Supplementary Material. The derived parameter α measures the degree to which a drug maintains SA following increases in unit price (FR / unit dose), and serves as an index of opioid reinforcement efficacy. Assignment to High and Low demand groups was based on a median split of α values.

Reinstatement. Assignment to High and Low reinstatement groups was based on a median split of reinstatement scores, defined using the formula: (active - inactive responses during reinstatement test) - (average of last 3 days of active - inactive responses during extinction). Differences in the reinstatement score was assessed using a 2-factor (sex x drug type) ANOVA, with a Šidák post-hoc test to determine within-factor differences. Active and inactive lever responses during saline and morphine-primed reinstatement testing were examined in males and females using a 3-factor (Sex x Reinstatement Drug x

Lever type) ANOVA, further analysis with sex collapsed were conducted using a 2-factor ANOVA and a Šidák post-hoc test to determine within-factor differences.

mPFC dissection

Rats were deep anesthetized with isoflurane before decapitation. Brains were removed and dissected on an ice-cold metal block. The mPFC from both hemispheres was isolated and aliquoted, flash-frozen in liquid nitrogen, and stored at -80°C.

RNA isolation and DNA transposition

Total RNA was isolated using the RNAqueous™-Micro Kit (Invitrogen) according to the manufacturer's protocol. Nuclei isolation and DNA transposition were carried out as previously described (*66*) with modifications. Briefly, flash-frozen mPFC was thawed in cold homogenization buffer (5 mM $CaCl_2$, 3 mM $Mg(AC)_2$, 10 mM Tris pH 7.8, 0.0167 mM PMSF, 0.167 mM β-mercaptoethanol, 1x proteinase inhibitor (cOmplete), 320 mM sucrose, 0.1 mM EDTA, 0.1% CA630), and homogenized using a Pellet Pestle motor and syringe. Equal volume of 50% iodixanol solution (5 mM $CaCl_2$, 3 mM $Mg(AC)_2$, 10 mM Tris pH 7.8, 0.017 mM PMSF, 0.17 mM β-mercaptoethanol, 1x proteinase inhibitor (cOmplete), 50% iodixanol) was added to homogenate to reach a final concentration of 25% iodixanol. 30% (5 mM $CaCl_2$, 3 mM $Mg(AC)_2$, 10 mM Tris pH 7.8, 0.017 mM PMSF, 0.17 mM β-mercaptoethanol, 1x proteinase inhibitor (cOmplete), 160 mM sucrose, 30% iodixanol) and 40% (5 mM $CaCl_2$, 3 mM $Mg(AC)_2$, 10 mM Tris pH 7.8, 0.017 mM PMSF, 0.17 mM β-mercaptoethanol, 1x proteinase inhibitor (cOmplete), 160 mM sucrose, 40% iodixanol) iodixanol solution were sequentially added under the 25% iodixanol solution layer. The 3-layer system was centrifuged in a swinging bucket centrifuge at 4255 x g for 30 min. After centrifugation, nuclei were isolated and collected from the 30%-40% iodixanol solution interface. Isolated nuclei were counted with trypan blue (0.4%) and 50,000 nuclei were transferred into a tube containing 1 ml ATAC-RSB (10 mM Tris pH 7.8, 10 mM NaCl, 3 mM $MgCl_2$) with 0.1% Tween-20. Nuclei were pelleted by centrifugation at 500 x g for 10 min. All steps above were conducted on ice or at 4°C. Nuclei were resuspended in transposition mix (25 µL 2x TD buffer (Illumina), 16.5 µL PBS, 0.5 µL 10% Tween-20, 1% digitonin, 2.5 µL Tn5 transposase (Illumina), 5 µL H_2O), and incubated at 37°C for 30 min in a thermomixer at 1000 rpm. Transposed DNA was purified using MinElute Reaction Cleanup kit (Qiagen).

Library preparation and sequencing

For RNA-seq, total isolated RNA was quantified using the RiboGreen RNA Assay kit (Invitrogen) and assessed for quality using capillary electrophoresis (Agilent BioAnalyzer 2100; Agilent). Barcoded libraries were constructed for each sample using the TruSeq RNA v2 kit (Illumina). For ATAC-seq, isolated DNA was first quantified using the PicoGreen dsDNA Assay Kit (Invitrogen). ATAC-seq library preparation was performed in accordance with the ATAC-seq protocol as described by Buenrostro et al. (2015) (*67*). Libraries were assessed for quality using capillary electrophoresis (Agilent BioAnalyzer 2100; Agilent). RNA-seq and ATAC-seq libraries were size-selected for ~200 and 200~800 bp fragments, respectively. Selected libraries were sequenced at a depth of ~100 million reads per sample using NovaSeq 6000.

RNA- and ATAC-seq analysis

Raw sequencing reads were aligned to the Ensembl v90 rat reference genome (rn6) using HISAT2 (v2.2.1) (*68*). Differential gene expression analysis was performed in R (v4.0.2) using the DESeq2 package (*69*). MACS (v2.1.0) was utilized to assess sites (peaks) of

chromatin accessibility in ATAC-seq samples (*70*). MACS2 was run with parameters -p 1e-05 --nomodel --shift 100 --extsize 200. diffReps (*71*) was utilized with default parameters to find differential sites between the comparison groups. Differential sites were mapped to genes using the tool HOMER (PMID: 20513432) (*72*). Significance was set at absolute log2(Fold Change) > 0.32 and $p < 0.05$ for RNA-seq, $q < 0.05$ for ATAC-seq.

Weighted Gene Co-expression Network Analysis (WGCNA)

Sample expression values were normalized with variance stabilizing transformation (VST) using DESeq2. The biomaRt R package was used for extracting additional gene information, using the Ensembl Archive Release 104 (May 2021). The "removeBatchEffect" function from the limma package was used to remove the batch effect from the VST expression. WGCNA was used for module detection. In brief, the batch-adjusted VST expression was converted to an adjacency matrix using the "adjacency" function, with softPower=4. Topological overlap matrix similarity and dissimilarity was calculated using the "TOMsimilarity" function. Hierarchical clustering was performed on the adjacency matrix, using the "hclust" function (method="average"). Requiring a minimum module size of 30 genes, the hierarchical clustering was cut into modules using the "cutreeDynamic" function. Numeric labels of modules were converted to colors using the "labels2colors" function. The eigengenes of the modules was calculated using the "moduleEigengenes" function, followed by a hierarchical clustering of the dissimilarity of the module eigengenes. Closely related modules were then merged using the "mergeCloseModules" function.

Once modules were generated, Differential Gene Connectivity Analysis (DGCA) was performed using the DGCA package in R, to determine the differential connectivity between morphine and saline conditions. Over-representation of differential gene sets with gene-associated modules was done using a hypergeometric test. Gene regulatory networks were calculated using ARACNE AP (version 2016-04-01) on batch-adjusted VST expression values, with 100 bootstrap iterations. Mouse regulatory factors used in ARACNE were extracted from TRRUST (version2). Pearson correlation of module relationships to sample characteristics (i.e., "Behavior.Score") was generated using the "cor" function. Network graphs were generated in R using the ggraph package.

Ingenuity Pathway Analysis (IPA)

Differentially expressed genes (DEGs) were annotated by Ingenuity pathway Analysis (IPA; Qiagen) to identify relevant canonical pathways, molecular networks and cellular functions that showed significant alterations between comparison groups as previously described (*73*). Statistical significance ($p < 0.05$; $-\log(p) > 1.3$) was determined by Fisher's exact test.

Variance Partitioning Analysis

'variancePartition' package in R was used to compute the percentage variance explained by Paradigm and Vulnerability in the data set (*25*). Counts for each sample was loaded into R environment. For both male and female rats, we obtained the VST counts using DESeq2 for all genes. Batch effects were removed from the VST counts using the fitVarPartModel function. The formula for fitExtractVarPartModel was set to ~ (1|Vulnerability) + (1|Paradigm) where Vulnerability takes on the values 'Vulnerable' and 'Resilient' and Paradigm take on the values ICSS, Reinstatement and Demand. fitExtractVarPartModel function estimated the variation from Vulnerability differences for each gene across samples.

Heatmaps sorted by the percent variance in genes explained by Vulnerability show the expression level of the top 50 most variable genes across the 2 vulnerability groups 'Resilient' and 'Vulnerable' as well as the 3 paradigms Demand, ICSS and Reinstatement. Heatmaps were generated using the R package 'pheatmap'. Hierarchical clustering was applied for both rows and columns, and expression values were scaled for each row.

Rank-rank hypergeometric overlap (RRHO)

The RRHO method was used to evaluate overlap in gene signatures between human OUD patients (assayed in dorsolateral PFC (dlPFC) and nucleus accumbens (NAc) postmortem by RNA-seq) and morphine dependence in rats in this study in a threshold-free manner (*74*). DEG files from human OUD samples were obtained from Seney et al. (2021) (*75*). Briefly, we ranked differential gene expression in both datasets based on the signed -log(p-value), with the sign depending upon whether a gene was up or down-regulated. We implemented a sliding window approach to scan through genes iteratively in both gene lists and computed hyper-geometric test p-values for each window. The Benjamini-Yekutieli multiple hypothesis correction was applied to the p-values. The computed p-adj values were converted to -log (p-adj) values and represented as a heat map; color scale ranging from blue to red.

HOMER motif analysis

The program 'findMotifsGenome.pl' from the tool HOMER (PMID: 20513432) (*72*) was utilized to identify motifs of transcription factors among differential sites identified by diffReps (PMID: 23762400) (*71*) after applying an absolute log2(Fold Change) cutoff of 0.32 and a *q*-value cutoff of 0.05.

References

1. J. Strang, N. D. Volkow, L. Degenhardt, M. Hickman, K. Johnson, G. F. Koob, B. D. L. Marshall, M. Tyndall, S. L. Walsh, Opioid use disorder. *Nat Rev Dis Primers* **6** (2020).
2. K. E. Vowles, M. L. McEntee, P. S. Julnes, T. Frohe, J. P. Ney, D. N. Van Der Goes, Rates of opioid misuse, abuse, and addiction in chronic pain: a systematic review and data synthesis. *Pain* **156**, 569–576 (2015).
3. K. S. Kendler, S. L. Lönn, J. Ektor-Andersen, J. Sundquist, K. Sundquist, Risk factors for the development of opioid use disorder after first opioid prescription: a Swedish national study. *Psychol Med* **53**, 6223–6231 (2023).
4. C. Higgins, B. H. Smith, K. Matthews, Incidence of iatrogenic opioid dependence or abuse in patients with pain who were exposed to opioid analgesic therapy: a systematic review and meta-analysis. *Br J Anaesth* **120**, 1335–1344 (2018).
5. E. R. Gibney, C. M. Nolan, Epigenetics and gene expression. *Heredity (Edinb)* **105**, 4–13 (2010).
6. C. T. Werner, R. D. Altshuler, Y. Shaham, X. Li, Epigenetic mechanisms in drug relapse. *Biol Psychiatry* **89**, 331 (2021).
7. D. Baker-Andresen, Q. Zhao, X. Li, B. Jupp, R. Chesworth, A. J. Lawrence, T. W. Bredy, Persistent variations in neuronal DNA methylation following cocaine self-administration and protracted abstinence in mice. *Neuroepigenetics* **4**, 1–11 (2015).
8. W. M. Freeman, K. M. Patel, R. M. Brucklacher, M. E. Lull, M. Erwin, D. Morgan, D. C. S. Roberts, K. E. Vrana, Persistent Alterations in Mesolimbic Gene Expression with Abstinence from Cocaine Self-Administration. *Neuropsychopharmacology 2008 33:8* **33**, 1807–1817 (2008).
9. A. Sadakierska-Chudy, M. Frankowska, J. Jastrzębska, K. Wydra, J. Miszkiel, M. Sanak, M. Filip, Cocaine Administration and Its Withdrawal Enhance the Expression of Genes Encoding Histone-Modifying Enzymes and Histone Acetylation in the Rat Prefrontal Cortex. *Neurotox Res* **32**, 141–150 (2017).
10. G. Sadri-Vakili, V. Kumaresan, H. D. Schmidt, K. R. Famous, P. Chawla, F. M. Vassoler, R. P. Overland, E. Xia, C. E. Bass, E. F. Terwilliger, R. C. Pierce, J. H. J. Cha, Cocaine-Induced Chromatin Remodeling Increases Brain-Derived Neurotrophic Factor Transcription in the Rat Medial Prefrontal Cortex, Which Alters the Reinforcing Efficacy of Cocaine. *Journal of Neuroscience* **30**, 11735–11744 (2010).
11. C. J. Browne, R. Futamura, A. Minier-Toribio, E. M. Hicks, A. Ramakrishnan, F. J. Martínez-Rivera, M. Estill, A. Godino, E. M. Parise, A. Torres-Berrío, A. M. Cunningham, P. J. Hamilton, D. M. Walker, L. M.

Huckins, Y. L. Hurd, L. Shen, E. J. Nestler, Transcriptional signatures of heroin intake and relapse throughout the brain reward circuitry in male mice. *Sci Adv* **9** (2023).

12. J. R. DiFranza, J. A. Savageau, K. Fletcher, L. Pbert, J. O'Loughlin, A. D. McNeill, J. K. Ockene, K. Friedman, J. Hazelton, C. Wood, G. Dussault, R. J. Wellman, Susceptibility to nicotine dependence: the Development and Assessment of Nicotine Dependence in Youth 2 study. *Pediatrics* **120** (2007).
13. J. O'Loughlin, J. DiFranza, R. F. Tyndale, G. Meshefedjian, E. McMillan-Davey, P. B. S. Clarke, J. Hanley, G. Paradis, Nicotine-dependence symptoms are associated with smoking frequency in adolescents. *Am J Prev Med* **25**, 219–225 (2003).
14. M. A. Schuckit, T. L. Smith, J. Kalmijn, The search for genes contributing to the low level of response to alcohol: patterns of findings across studies. *Alcohol Clin Exp Res* **28**, 1449–1458 (2004).
15. K. S. Nishida, T. Y. Park, B. H. Lee, R. J. Ursano, K. H. Choi, Individual differences in initial morphine sensitivity as a predictor for the development of opiate addiction in rats. *Behavioural brain research* **313**, 315–323 (2016).
16. Y. Swain, P. Muelken, A. Skansberg, D. Lanzdorf, Z. Haave, M. G. LeSage, J. C. Gewirtz, A. C. Harris, Higher anhedonia during withdrawal from initial opioid exposure is protective against subsequent opioid self-administration in rats. *Psychopharmacology (Berl)* **237**, 2279 (2020).
17. M. E. Carroll, A. D. Morgan, W. J. Lynch, U. C. Campbell, N. K. Dess, Intravenous cocaine and heroin self-administration in rats selectively bred for differential saccharin intake: phenotype and sex differences. *Psychopharmacology (Berl)* **161**, 304–313 (2002).
18. B. S. Bentzley, K. M. Fender, G. Aston-Jones, The behavioral economics of drug self-administration: a review and new analytical approach for within-session procedures. *Psychopharmacology (Berl)* **226**, 113–125 (2013).
19. W. K. Bickel, M. W. Johnson, M. N. Koffarnus, J. MacKillop, J. G. Murphy, The Behavioral Economics of Substance Use Disorders: reinforcement pathologies and their repair. *Annu Rev Clin Psychol* **10**, 641 (2014).
20. I. Fredriksson, M. Venniro, D. J. Reiner, J. J. Chow, J. M. Bossert, Y. Shaham, Animal Models of Drug Relapse and Craving after Voluntary Abstinence: A Review. *Pharmacol Rev* **73**, 1050–1083 (2021).
21. D. E. Moorman, M. H. James, E. M. McGlinchey, G. Aston-Jones, Differential roles of medial prefrontal subregions in the regulation of drug seeking. *Brain Res* **1628**, 130–146 (2015).
22. M. C. Van den Oever, S. Spijker, A. B. Smit, T. J. De Vries, Prefrontal cortex plasticity mechanisms in drug seeking and relapse. *Neurosci Biobehav Rev* **35**, 276–284 (2010).
23. A. O. Ceceli, C. W. Bradberry, R. Z. Goldstein, The neurobiology of drug addiction: cross-species insights into the dysfunction and recovery of the prefrontal cortex. *Neuropsychopharmacology 2021 47:1* **47**, 276–291 (2021).
24. P. Langfelder, R. Luo, M. C. Oldham, S. Horvath, Is My Network Module Preserved and Reproducible? *PLoS Comput Biol* **7**, e1001057 (2011).
25. G. E. Hoffman, E. E. Schadt, variancePartition: Interpreting drivers of variation in complex gene expression studies. *BMC Bioinformatics* **17**, 1–13 (2016).
26. T. Fuller, P. Langfelder, A. Presson, S. Horvath, Review of Weighted Gene Coexpression Network Analysis. *Handbook of Statistical Bioinformatics*, 369–388 (2011).
27. K. Scott, R. O'Rourke, A. Gillen, B. Appel, Prdm8 regulates pMN progenitor specification for motor neuron and oligodendrocyte fates by modulating the Shh signaling response. *Development* **147** (2020).
28. H. Fu, S. Kesari, J. Cai, Tcf7l2 is Tightly Controlled During Myelin Formation. *Cell Mol Neurobiol* **32**, 345 (2012).
29. S. Zhang, X. Zhu, X. Gui, C. Croteau, L. Song, J. Xu, A. Wang, P. Bannerman, F. Guo, Sox2 Is Essential for Oligodendroglial Proliferation and Differentiation during Postnatal Brain Myelination and CNS Remyelination. *The Journal of Neuroscience* **38**, 1802 (2018).
30. A. Benraiss, J. N. Mariani, A. Tate, P. M. Madsen, K. M. Clark, K. A. Welle, R. Solly, L. Capellano, K. Bentley, D. Chandler-Militello, S. A. Goldman, A TCF7L2-responsive suppression of both homeostatic and compensatory remyelination in Huntington disease mice. *Cell Rep* **40** (2022).
31. R. K. Tiwari, V. Sharma, R. K. Pandey, S. S. Shukla, Nicotine Addiction: Neurobiology and Mechanism. *J Pharmacopuncture* **23**, 1 (2020).
32. R. A. Wise, M. A. Robble, Dopamine and Addiction. *Annu Rev Psychol* **71**, 79–106 (2020).
33. K. D. Ersche, C. Meng, H. Ziauddeen, J. Stochl, G. B. Williams, E. T. Bullmore, T. W. Robbins, Brain networks underlying vulnerability and resilience to drug addiction. *Proc Natl Acad Sci U S A* **117**, 15253–15261 (2020).
34. R. Miela, W. J. Cubała, D. W. Mazurkiewicz, K. Jakuszkowiak-Wojten, The neurobiology of addiction. A vulnerability/resilience perspective. *Eur J Psychiatry* **32**, 139–148 (2018).
35. S. Spijker, S. W. J. Houtzager, M. C. M. De Gunst, W. P. H. De Boer, A. N. M. Schoffelmeer, A. B. Smit, Morphine exposure and abstinence define specific stages of gene expression in the rat nucleus accumbens. *The FASEB journal : official publication of the Federation of American Societies for Experimental Biology* **18**, 848–850 (2004).

36. F. Di Tullio, M. Schwarz, H. Zorgati, S. Mzoughi, E. Guccione, The duality of PRDM proteins: epigenetic and structural perspectives. *FEBS J* **289**, 1256–1275 (2022).
37. B. Yalçın, M. B. Pomrenze, K. Malacon, R. Drexler, A. E. Rogers, K. Shamardani, I. J. Chau, K. R. Taylor, L. Ni, D. Contreras-Esquivel, R. C. Malenka, M. Monje, Myelin plasticity in the ventral tegmental area is required for opioid reward. *Nature 2024 630:8017* **630**, 677–685 (2024).
38. P. O. Gaudreault, S. G. King, P. Malaker, N. Alia-Klein, R. Z. Goldstein, Whole-brain white matter abnormalities in human cocaine and heroin use disorders: association with craving, recency, and cumulative use. *Molecular Psychiatry 2022 28:2* **28**, 780–791 (2022).
39. R. Fan, L. M. Schrott, T. Arnold, S. Snelling, M. Rao, D. Graham, A. Cornelius, N. L. Korneeva, Chronic oxycodone induces axonal degeneration in rat brain. *BMC Neurosci* **19**, 1–20 (2018).
40. E. R. Butelman, R. Z. Goldstein, C. A. Nwaneshiudu, K. Girdhar, P. Roussos, S. J. Russo, N. Alia-Klein, Neuroimmune Mechanisms of Opioid Use Disorder and Recovery: Translatability to Human Studies, and Future Research Directions. *Neuroscience* **528**, 102–116 (2023).
41. M. L. Seney, S. M. Kim, J. R. Glausier, M. A. Hildebrand, X. Xue, W. Zong, J. Wang, M. A. Shelton, B. D. N. Phan, C. Srinivasan, A. R. Pfenning, G. C. Tseng, D. A. Lewis, Z. Freyberg, R. W. Logan, Transcriptional Alterations in Dorsolateral Prefrontal Cortex and Nucleus Accumbens Implicate Neuroinflammation and Synaptic Remodeling in Opioid Use Disorder. *Biol Psychiatry* **90**, 550–562 (2021).
42. L. N. Eidson, A. Z. Murphy, Inflammatory mediators of opioid tolerance: Implications for dependency and addiction. *Peptides (N.Y.)* **115**, 51–58 (2019).
43. J. Cuitavi, J. V. Torres-Pérez, J. D. Lorente, Y. Campos-Jurado, P. Andrés-Herrera, A. Polache, C. Agustín-Pavón, L. Hipólito, Crosstalk between Mu-Opioid receptors and neuroinflammation: Consequences for drug addiction and pain. *Neurosci Biobehav Rev* **145**, 105011 (2023).
44. Y. Yang, L. Guo, L. Chen, B. Gong, D. Jia, Q. Sun, Nuclear transport proteins: structure, function, and disease relevance. *Signal Transduction and Targeted Therapy 2023 8:1* **8**, 1–29 (2023).
45. L. Chen, Y. Wang, J. Lin, Z. Song, Q. Wang, W. Zhao, Y. Wang, X. Xiu, Y. Deng, X. Li, Q. Li, X. Wang, J. Li, X. Liu, K. Liu, J. Zhou, K. Li, Y. Liu, S. Liao, Q. Deng, C. Xu, Q. Sun, S. Wu, K. Zhang, M. X. Guan, T. Zhou, F. Sun, X. Cai, C. Huang, G. Shan, Exportin 4 depletion leads to nuclear accumulation of a subset of circular RNAs. *Nature Communications 2022 13:1* **13**, 1–18 (2022).
46. H. Yu, B. Xie, J. Zhang, Y. Luo, E. Galaj, X. Zhang, Q. Shen, Y. Liu, B. Cong, D. Wen, C. Ma, The role of circTmeff-1 in incubation of context-induced morphine craving. *Pharmacol Res* **170**, 105722 (2021).
47. S. E. Sillivan, A. Gillespie, Circular RNA regulation and function in drug seeking phenotypes. *Molecular and Cellular Neuroscience* **125**, 103841 (2023).
48. R. Massart, S. Dymov, M. Millecamps, M. Suderman, S. Gregoire, K. Koenigs, S. Alvarado, M. Tajerian, L. S. Stone, M. Szyf, Overlapping signatures of chronic pain in the DNA methylation landscape of prefrontal cortex and peripheral T cells. *Scientific Reports 2016 6:1* **6**, 1–13 (2016).
49. A. Raj, A. van Oudenaarden, Nature, Nurture, or Chance: Stochastic Gene Expression and Its Consequences. *Cell* **135**, 216–226 (2008).
50. S. Sukumaran, R. R. Almon, D. C. DuBois, W. J. Jusko, Circadian rhythms in gene expression: Relationship to physiology, disease, drug disposition and drug action. *Adv Drug Deliv Rev* **62**, 904–917 (2010).
51. J. Z. Li, B. G. Bunney, F. Meng, M. H. Hagenauer, D. M. Walsh, M. P. Vawter, S. J. Evans, P. V. Choudary, P. Cartagena, J. D. Barchas, A. F. Schatzberg, E. G. Jones, R. M. Myers, S. J. Watson, H. Akil, W. E. Bunney, Circadian patterns of gene expression in the human brain and disruption in major depressive disorder. *Proc Natl Acad Sci U S A* **110**, 9950–9955 (2013).
52. L. López-Maury, S. Marguerat, J. Bähler, Tuning gene expression to changing environments: from rapid responses to evolutionary adaptation. *Nat Rev Genet* **9**, 583–593 (2008).
53. C. J. Browne, A. Godino, M. Salery, E. J. Nestler, Epigenetic Mechanisms of Opioid Addiction. *Biol Psychiatry* **87**, 22–33 (2020).
54. J. L. Zhou, G. de Guglielmo, A. J. Ho, M. Kallupi, N. Pokhrel, H. R. Li, A. S. Chitre, D. Munro, P. Mohammadi, L. L. G. Carrette, O. George, A. A. Palmer, G. McVicker, F. Telese, Single-nucleus genomics in outbred rats with divergent cocaine addiction-like behaviors reveals changes in amygdala GABAergic inhibition. *Nature Neuroscience 2023 26:11* **26**, 1868–1879 (2023).
55. M. Foretz, B. Guigas, B. Viollet, Metformin: update on mechanisms of action and repurposing potential. *Nature Reviews Endocrinology 2023 19:8* **19**, 460–476 (2023).
56. N. Sanadgol, M. Barati, F. Houshmand, S. Hassani, T. Clarner, M. shahlaei, F. Golab, Metformin accelerates myelin recovery and ameliorates behavioral deficits in the animal model of multiple sclerosis via adjustment of AMPK/Nrf2/mTOR signaling and maintenance of endogenous oligodendrogenesis during brain self-repairing period. *Pharmacol Rep* **72**, 641–658 (2020).
57. J. Kosaraju, M. Seegobin, A. Gouveia, C. Syal, S. N. Sarma, K. J. Lu, J. Ilin, L. He, F. E. Wondisford, D. Lagace, Y. De Repentigny, R. Kothary, J. Wang, Metformin promotes CNS remyelination and improves social interaction following focal demyelination through CBP Ser436 phosphorylation. *Exp Neurol* **334** (2020).

58. A. Chan, A. Willard, S. Mulloy, N. Ibrahim, A. Sciaccotta, M. Schonfeld, S. M. Spencer, Metformin in nucleus accumbens core reduces cue-induced cocaine seeking in male and female rats. *Addiction biology* **27** (2022).
59. N. A. Holtz, A. K. Radke, N. E. Zlebnik, A. C. Harris, M. E. Carroll, Intracranial self-stimulation reward thresholds during morphine withdrawal in rats bred for high (HiS) and low (LoS) saccharin intake. *Brain Res* **1602**, 119 (2015).
60. J. Liu, G. Schulteis, Brain reward deficits accompany naloxone-precipitated withdrawal from acute opioid dependence. *Pharmacol Biochem Behav* **79**, 101–108 (2004).
61. J. Feng, M. Wilkinson, X. Liu, I. Purushothaman, D. Ferguson, V. Vialou, I. Maze, N. Shao, P. Kennedy, J. W. Koo, C. Dias, B. Laitman, V. Stockman, Q. LaPlant, M. E. Cahill, E. J. Nestler, L. Shen, Chronic cocaine-regulated epigenomic changes in mouse nucleus accumbens. *Genome Biol* **15** (2014).
62. G. E. Hodes, M. L. Pfau, I. Purushothaman, H. F. Ahn, S. A. Golden, D. J. Christoffel, J. Magida, A. Brancato, A. Takahashi, M. E. Flanigan, C. Menard, H. Aleyasin, J. W. Koo, Z. S. Lorsch, J. Feng, M. Heshmati, M. Wang, G. Turecki, R. Neve, B. Zhang, L. Shen, E. J. Nestler, S. J. Russo, Sex Differences in Nucleus Accumbens Transcriptome Profiles Associated with Susceptibility versus Resilience to Subchronic Variable Stress. *Journal of Neuroscience* **35**, 16362–16376 (2015).
63. M. Li, P. Xu, Y. Xu, H. Teng, W. Tian, Q. Du, M. Zhao, Dynamic expression changes in the transcriptome of the prefrontal cortex after repeated exposure to cocaine in mice. *Front Pharmacol* **8**, 142 (2017).
64. D. M. Walker, H. M. Cates, Y. H. E. Loh, I. Purushothaman, A. Ramakrishnan, K. M. Cahill, C. K. Lardner, A. Godino, H. G. Kronman, J. Rabkin, Z. S. Lorsch, P. Mews, M. A. Doyle, J. Feng, B. Labonté, J. W. Koo, R. C. Bagot, R. W. Logan, M. L. Seney, E. S. Calipari, L. Shen, E. J. Nestler, Cocaine Self-administration Alters Transcriptome-wide Responses in the Brain's Reward Circuitry. *Biol Psychiatry* **84**, 867–880 (2018).
65. Y. Swain, P. Muelken, M. G. LeSage, J. C. Gewirtz, A. C. Harris, Locomotor activity does not predict individual differences in morphine self-administration in rats. *Pharmacol Biochem Behav* **166**, 48 (2018).
66. M. R. Corces, A. E. Trevino, E. G. Hamilton, P. G. Greenside, N. A. Sinnott-Armstrong, S. Vesuna, A. T. Satpathy, A. J. Rubin, K. S. Montine, B. Wu, A. Kathiria, S. W. Cho, M. R. Mumbach, A. C. Carter, M. Kasowski, L. A. Orloff, V. I. Risca, A. Kundaje, P. A. Khavari, T. J. Montine, W. J. Greenleaf, H. Y. Chang, An improved ATAC-seq protocol reduces background and enables interrogation of frozen tissues. *Nature Methods 2017 14:10* **14**, 959–962 (2017).
67. J. Buenrostro, B. Wu, H. Chang, W. Greenleaf, ATAC-seq: A Method for Assaying Chromatin Accessibility Genome-Wide. *Current protocols in molecular biology / edited by Frederick M. Ausubel ... [et al.]* **109**, 21.29.1 (2015).
68. D. Kim, J. M. Paggi, C. Park, C. Bennett, S. L. Salzberg, Graph-Based Genome Alignment and Genotyping with HISAT2 and HISAT-genotype. *Nat Biotechnol* **37**, 907 (2019).
69. M. I. Love, W. Huber, S. Anders, Moderated estimation of fold change and dispersion for RNA-seq data with DESeq2. *Genome Biol* **15** (2014).
70. Y. Zhang, T. Liu, C. A. Meyer, J. Eeckhoute, D. S. Johnson, B. E. Bernstein, C. Nusbaum, R. M. Myers, M. Brown, W. Li, X. S. Liu, Model-based Analysis of ChIP-Seq (MACS). *Genome Biology 2008 9:9* **9**, 1–9 (2008).
71. L. Shen, N.-Y. Shao, X. Liu, I. Maze, J. Feng, E. J. Nestler, diffReps: Detecting Differential Chromatin Modification Sites from ChIP-seq Data with Biological Replicates. *PLoS One* **8**, e65598 (2013).
72. S. Heinz, C. Benner, N. Spann, E. Bertolino, Y. C. Lin, P. Laslo, J. X. Cheng, C. Murre, H. Singh, C. K. Glass, Simple combinations of lineage-determining transcription factors prime cis-regulatory elements required for macrophage and B cell identities. *Mol Cell* **38**, 576–589 (2010).
73. A. Barks, S. J. B. Fretham, M. K. Georgieff, P. V. Tran, Early-Life Neuronal-Specific Iron Deficiency Alters the Adult Mouse Hippocampal Transcriptome. *Journal of Nutrition* **148**, 1521–1528 (2018).
74. S. B. Plaisier, R. Taschereau, J. A. Wong, T. G. Graeber, Rank–rank hypergeometric overlap: identification of statistically significant overlap between gene-expression signatures. *Nucleic Acids Res* **38**, e169 (2010).
75. M. L. Seney, S. M. Kim, J. R. Glausier, M. A. Hildebrand, X. Xue, W. Zong, J. Wang, M. A. Shelton, B. D. N. Phan, C. Srinivasan, A. R. Pfenning, G. C. Tseng, D. A. Lewis, Z. Freyberg, R. W. Logan, Transcriptional Alterations in Dorsolateral Prefrontal Cortex and Nucleus Accumbens Implicate Neuroinflammation and Synaptic Remodeling in Opioid Use Disorder. *Biol Psychiatry* **90**, 550–562 (2021).

Acknowledgments

Acknowledgments follow the references and notes section but are not numbered. They should include the following information in the order listed below. Each section must be a **separate paragraph** and the heading in bold. Please use the subhead and boldface layout as shown below.).

If applicable, begin the section with text that acknowledges non-author contributions. (Note this section does not have a general heading).

Funding:
NIH/NIDA grant U01 DA051993 (JCG, ACH)
Hennepin Healthcare Research Institute Career Development Award (ACH)
University of Minnesota Doctoral Dissertation Fellowship (SXL)

Author contributions:

Conceptualization: JCG, ACH
Methodology: JCG, ACH, PVT, LS, JRS, SXL
Investigation:
Data curation: AR, MSE
Formal analysis: SXL, ACH
Visualization: SXL, AR, MSE, JRS, ACH
Supervision: JCG, ACH, PVT, LS, JRS, MGL
Writing—original draft: SXL, JCG, ACH
Writing—review & editing: SXL, PM, ZLM, AR, MSE, MGL, JRS, LS, PVT, ACH, JCG

Competing interests: All other authors declare they have no competing interests.

Data and materials availability: Sequencing data will be uploaded to GEO upon acceptance for publication and an accession number will be included in the published version of the article.

Figures and Tables

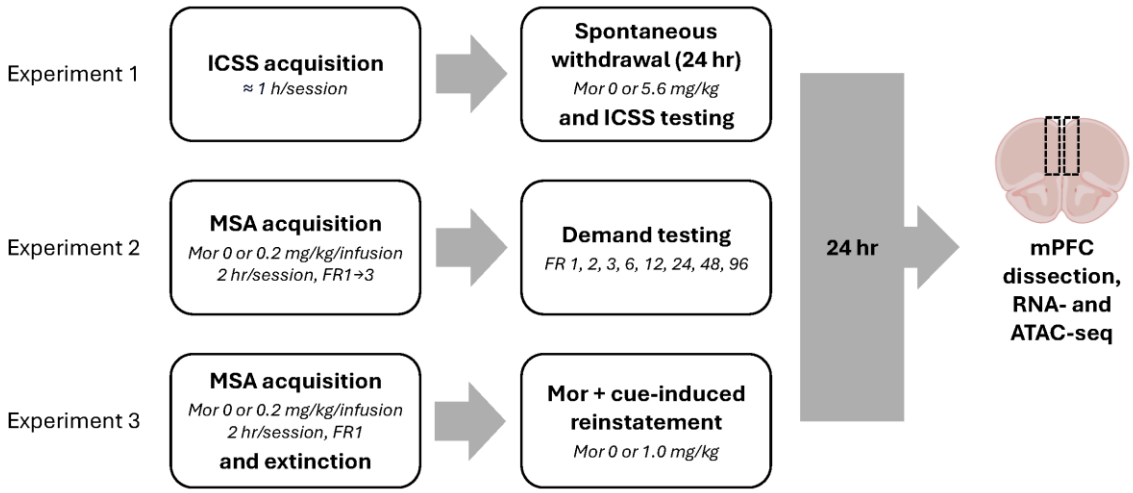

Fig. 1. Experimental design. Timeline of the three behavioral paradigms and mPFC collection is shown.

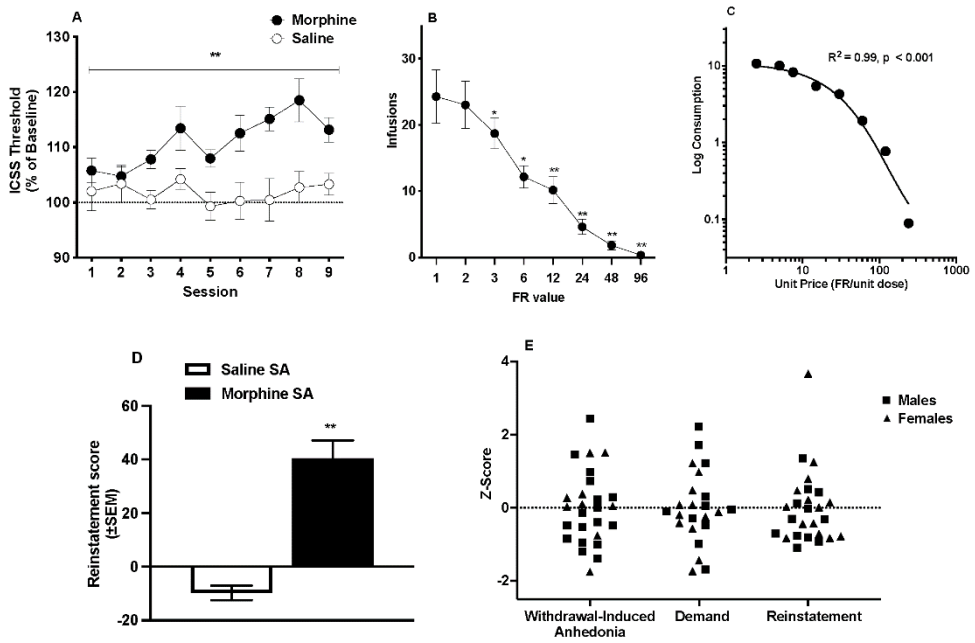

Fig. 2. Male and female rats exhibit individual difference in vulnerability in three behavioral paradigms. (A) ICSS thresholds (% Baseline, Mean ± SEM) during spontaneous morphine withdrawal. ** Different from Saline (main effect), $p < 0.0001$. **(B)** Infusions at each FR (Mean ± SEM) during demand testing. *,** Different from FR 1, $p < 0.05$ or 0.01. **(C)** Exponential demand function for morphine during demand testing. **(D)** Reinstatement scores (Mean ± SEM) during the reinstatement test following morphine or saline SA. ** Different from saline SA, $p < 0.01$. Data are collapsed across sex in Figs 1A – 1D because there were no significant effects of sex in any behavioral model. **(E)** Z-score distribution for individual morphine rats shown in panels (A)-(D).

.

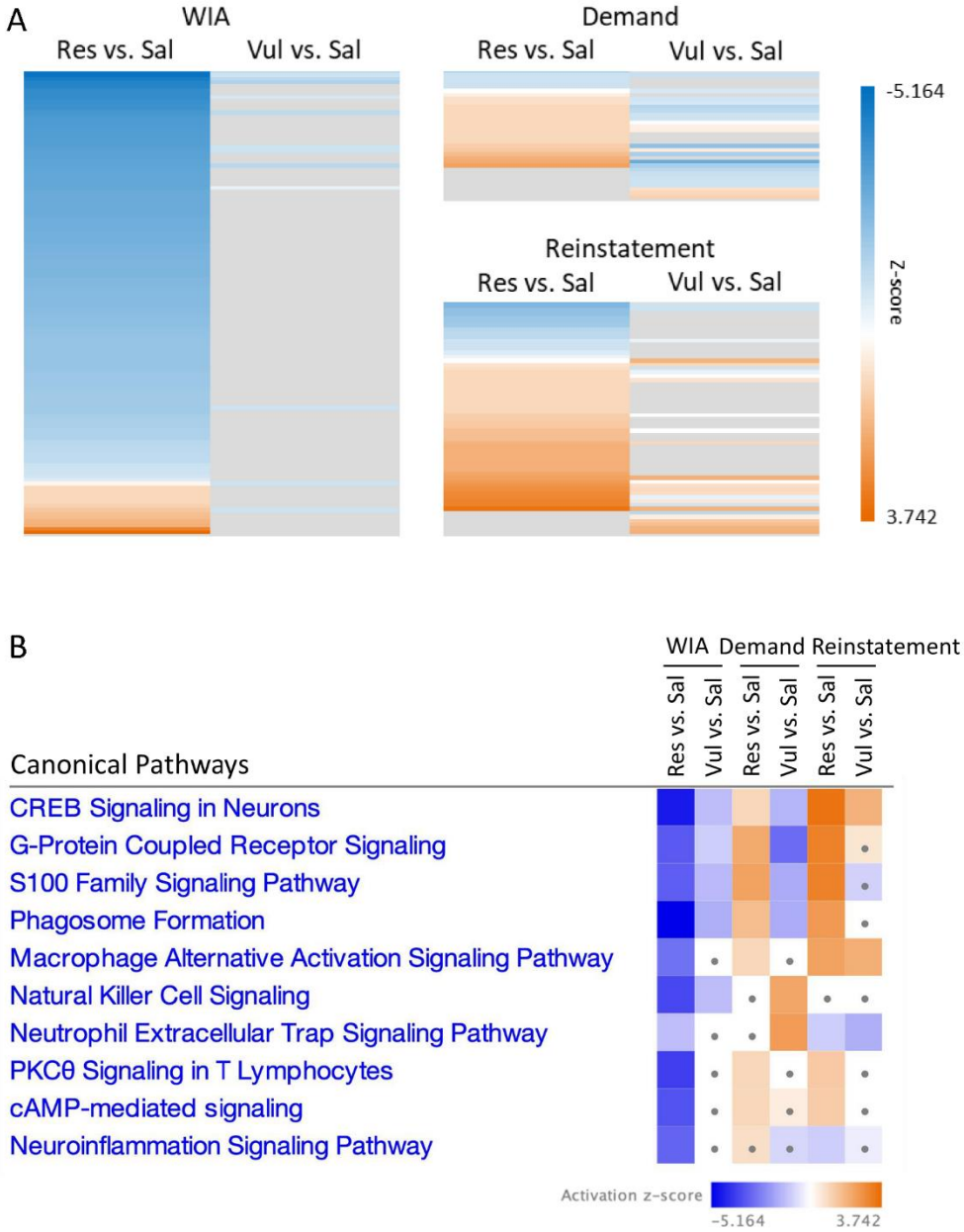

Fig. 3. Resilient male rats showed greater changes in IPA canonical pathways. (A) Heatmaps of all canonical pathways with detectable alteration in at least one comparison group. Each line represents one pathway. **(B)** Top 10 canonical pathways ranked by z-score. Grey, z-score = N/A; Square with a dot, absolute z-score < 1.

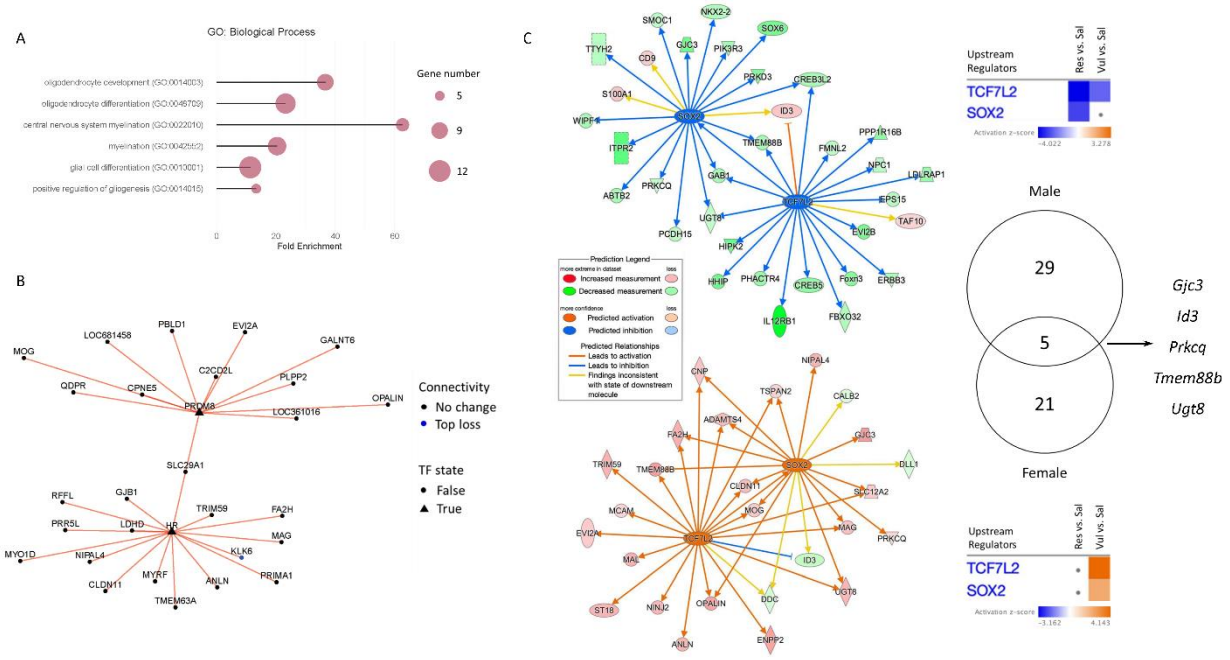

Fig. 4. Myelination/oligodendrocyte processes exhibited weaker activities in resilient groups in WIA rats in both sexes with distinct molecular mechanisms. (A) A WGCNA "saddlebrown" module with decreased connectivity in Morphine rats showed enrichment of genes functioning in oligodendrocyte processes and myelination. **(B)** ARACNe analyses of genes in the "saddlebrown" module. **(C)** IPA upstream regulator analysis predicted the activity of TCF7L2 and SOX2 with more inhibition in resilient WIA males, and with more activation in vulnerable WIA females. Square with a dot, absolute z-score < 1. Venn diagram showing 5 overlapping genes between WIA resilient male and vulnerable female TCF7L2 and SOX2 networks.

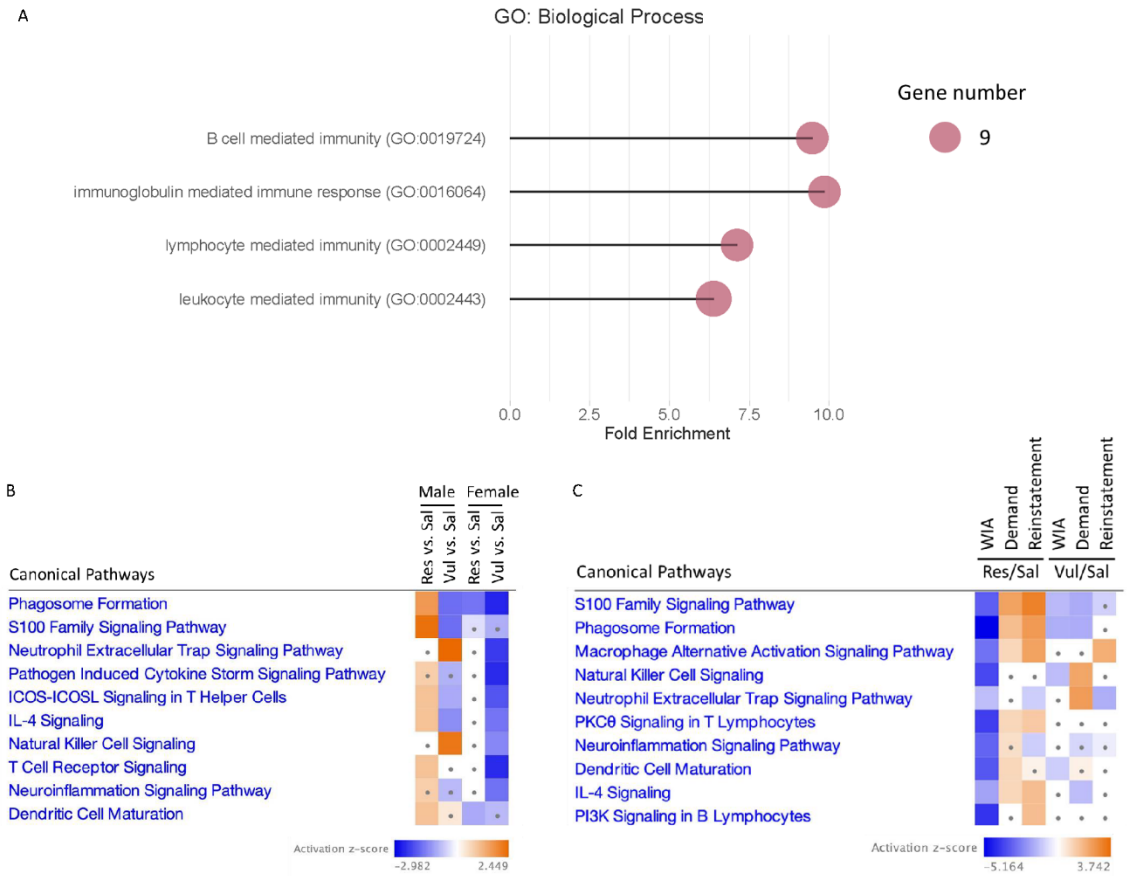

Fig. 5. Processes associated with neuroinflammation exhibited stronger activities in resilient groups in Demand rats in both sexes with distinct molecular mechanisms. (A) A WGCNA "white" module with decreased connectivity in Morphine rats showed enrichment of genes functioning in immune response/inflammation. **(B)** IPA analysis of top 10 neuroinflammation-associated pathways in Demand male and female resilient and vulnerable animals. **(C)** IPA analysis of top 10 neuroinflammation-associated pathways in male resilient and vulnerable animals in the WIA, Demand, and Reinstatement paradigms. Square with a dot, absolute z-score < 1.

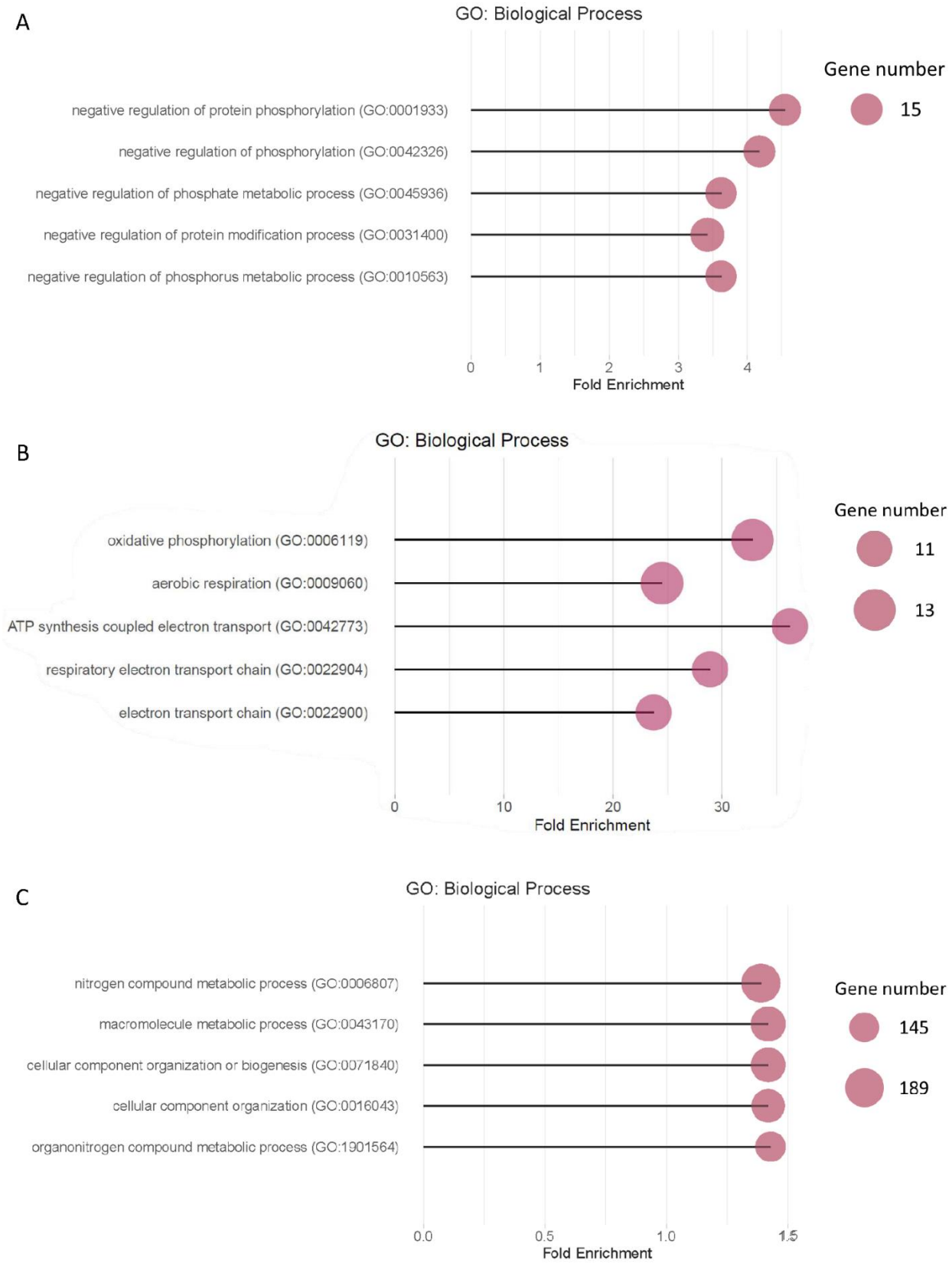

Fig. 6. Metabolism-associated modules were negatively correlated with the degree of resilience in male rats. (A) A WGCNA "darkgreen" module with decreased connectivity in Morphine rats in the Reinstatement paradigm showed enrichment of genes functioning in metabolic processes. This module was also negatively

correlated with reinstatement scores in male morphine rats. **(B, C)** WGCNA "darkgreen" **(B)** and "megenta" **(C)** Demand.Morphine modules that showed enrichment of genes functioning in metabolism were negatively correlated with elasticity of Demand (α) in male rats.

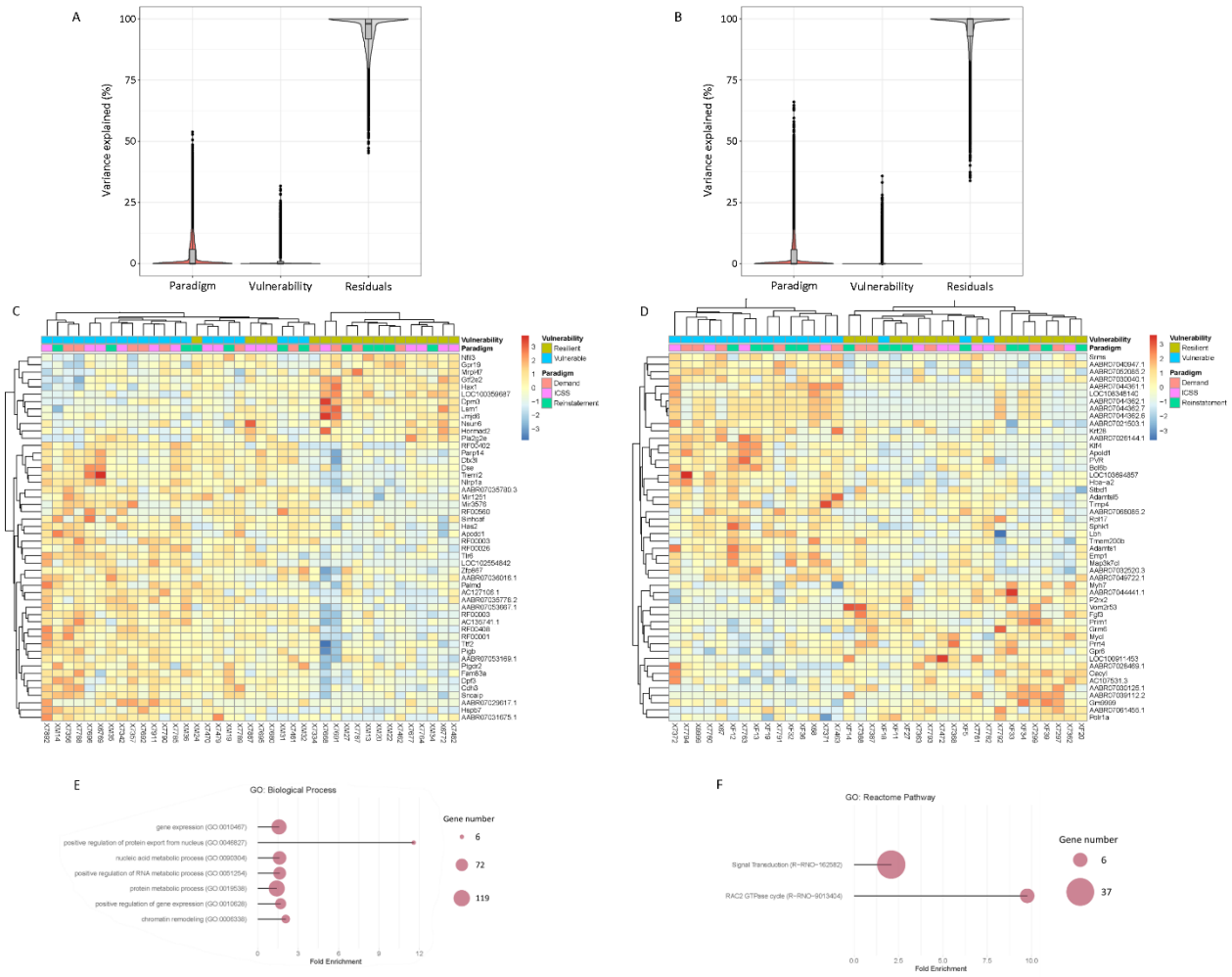

Fig. 7. Variance partitioning analyses for variations in gene expression attributed to vulnerability across 3 paradigms. (A, B) Violin plots showing the percentage of variance explained by paradigm, vulnerability, or residuals in male **(A)** and female **(B)** rats. **(C, D)** Heatmaps of clusters of the top 50 genes whose expression levels were explained by vulnerability in male **(C)** and female **(D)** rats. **(E)** Genes with greater than 10% of the variance explained by vulnerability in males were associated with regulations of gene expression. **(F)** Genes with greater than 10% of the variance explained by vulnerability in females were associated with cell signaling.

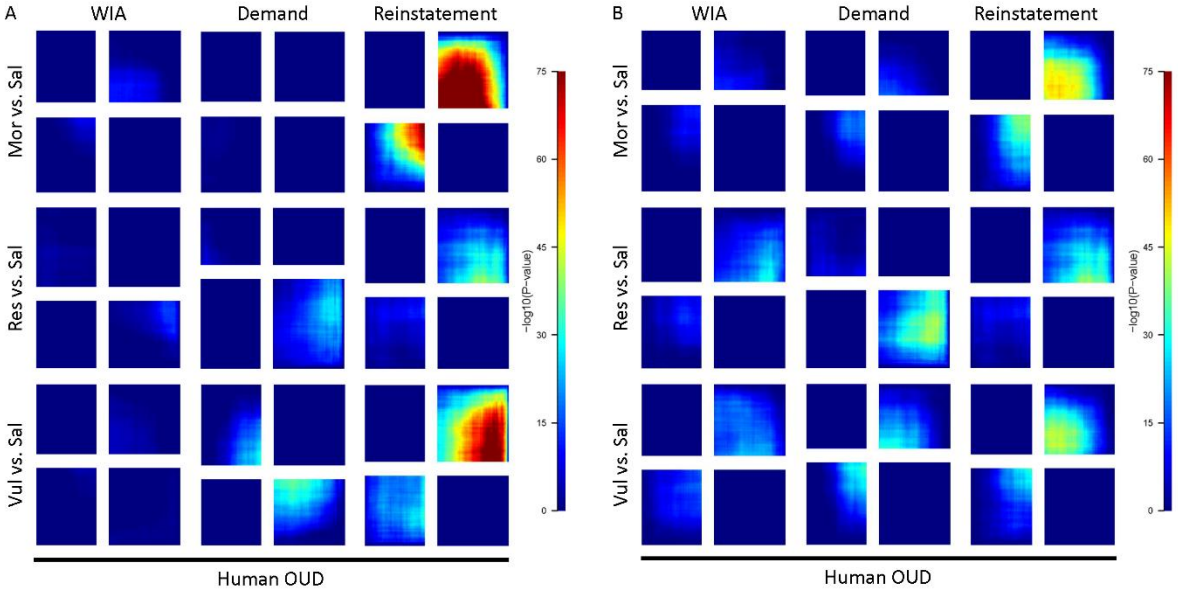

Fig. 8. Correlation of gene expression between humans and animal models. RRHO comparing gene expression patterns in the NAc of human OUD patients vs. controls and morphine-exposed, resilient, or vulnerable rats vs. control rats in males **(A)** and females **(B)** in 3 paradigms.

A

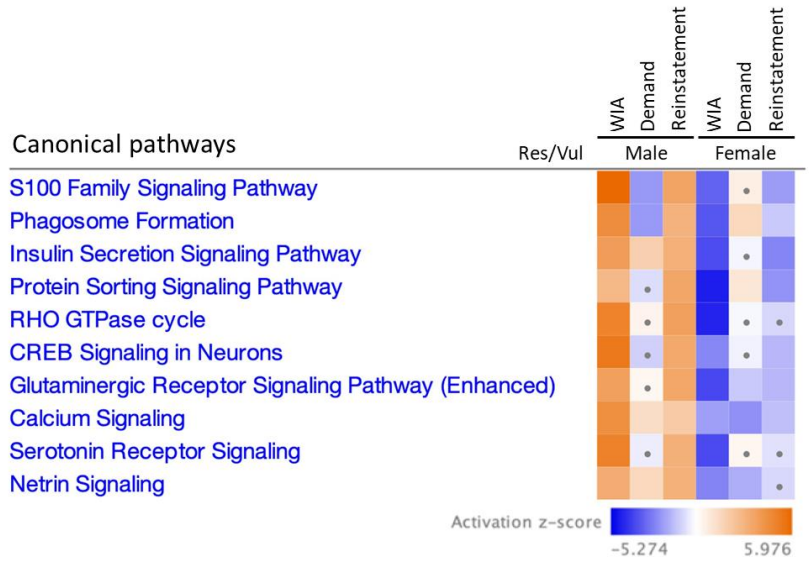

B

TF family	TFs	WIA			Demand			Reinstatement		
		Res vs. Vul	Res vs. Sal	Vul vs. Sal	Res vs. Vul	Res vs. Sal	Vul vs. Sal	Res vs. Vul	Res vs. Sal	Vul vs. Sal
AP-1	Fra2		x	x		x	x		x	
	Fos		x	x		x	x		x	
	Fra1		x	x		x	x			
	Atf3		x	x		x	x		x	
	JunB		x	x		x			x	
	AP-1		x	x		x	x		x	
	Fosl2		x	x		x	x		x	
	Jun-AP1		x	x		x	x			
	BATF			x		x			x	
MEF2	Mef2a		x		x			x		
	Mef2b						x	x		
	Mef2c				x			x		
	Mef2d		x		x		x	x		
bHLH	Atoh1				x		x			
	NeuroG2				x					
	NeuroD1				x					
	BHLHA15				x					
	Asl11				x					
	TCF4				x					
	Twist2				x					
	Npas4							x		
NR	PGR								x	x
	GRE								x	x
	ARE									x
Zf	Zic							x		
	Zfp57									x
	ZNF7									x
	ZNF415									x
	ZNF264									x
T-box	Tbr1							x		
	Tbx21							x		
	Tbet							x		
Others	HRE							x		
	Bach2			x		x				

Fig. 9. Common and unique gene expression regulatory mechanisms across paradigms revealed by ATAC-seq. (A) IPA canonical pathway analysis of Res vs. Vul differential chromatin accessibility sites showed opposite mechanisms between sexes. **(B)** HOMER motif analysis for male Res vs. Vul, Res vs. Sal, and

Vul vs. Sal ATAC-seq data. Top 10 significantly enriched motifs and their families were shown (indicated with “x”).